

SPECTROPHOTOMETRIC DATA OF THE CENTRAL STAR OF THE LARGE MAGELLANIC CLOUD PLANETARY NEBULA N66: QUANTITATIVE ANALYSIS OF ITS WN-TYPE SPECTRUM¹

M. PEÑA,^{2,3,4} W.-R. HAMANN,⁵ L. KOESTERKE,⁵ J. MAZA,^{3,6} R. H. MÉNDEZ,⁷ M. PEIMBERT,²
M. T. RUIZ^{3,6} AND S. TORRES-PEIMBERT²

Received 1997 May 22; accepted 1997 July 23

ABSTRACT

Hubble Space Telescope, *IUE*, and ground-based observations of the central star of the LMC planetary nebula N66 (CS N66), obtained in different epochs, are presented. Since 1990, CS N66 has displayed remarkable short- and long-term spectroscopic and photometric changes amounting to more than 3 mag in the optical. Expanding model atmospheres have been constructed to fit observations from different epochs. Fits provide the chemical composition, the fundamental stellar parameters L_* , T_* , R_* , the mass-loss rate, and the wind velocity. From our best models we find that CS N66 is a very luminous He star ($X/Y \leq 0.1$), with a small amount of N, undergoing a violent and unstable mass-loss event. The photospheric chemical abundances correspond to the equilibrium CNO nuclear burning values, while the nebula has a normal chemical composition. Models fitting data from different epochs indicate that the fundamental stellar parameters remain constant with time, with values $\log(L_*/L_\odot) = 4.53 \pm 0.10$, $T_* = 93,300$ K, and $R_* = 0.71 R_\odot$. The short- and long-term stellar variations are produced by large changes in the mass-loss rate, which varies by large factors, from $\dot{M} \leq 8 \times 10^{-7} M_\odot \text{ yr}^{-1}$ in 1983 (preoutburst epoch) to $\dot{M} = 2.5 \times 10^{-5} M_\odot \text{ yr}^{-1}$ in early 1995 (maximum stellar brightness). No evidence was found to support the suggestion that the outburst was due to a late thermal pulse. We propose that the event taking place in CS N66 was produced by an atmospheric instability similar to that triggering the giant eruptions of Population I luminous blue variable stars. The possible mechanism causing the atmospheric instability is briefly discussed.

Subject headings: Magellanic Clouds — planetary nebulae: individual (N66) — stars: evolution — stars: mass loss — stars: Wolf-Rayet

1. INTRODUCTION

N66 (also known as WS 35 and SMP 83) is a well-known type I planetary nebula (PN) in the LMC with a high ionization degree (see Peimbert 1978 for a description of PN types). Nebular chemical abundances (see, e.g., Peña et al. 1995; Dopita et al. 1993) indicate a moderately He- and N-rich nebula, with low C abundance. High spatial resolution images, obtained with the *Hubble Space Telescope* (*HST*), indicate a bipolar nebula with a highly filamentary structure (Dopita et al. 1993; Vassiliadis 1996).

Sanduleak (1977) noticed that N66 and the irregular variable HV 5967 are one and the same. Nail & Shapley (1955) found a variation range $\Delta m \approx 0.9$ mag for HV 5967. N66 was observed by several authors after Nail & Shapley's work, but no further variations were reported in the literature until 1990. In the last 7 years the central star of N66

(hereafter CS N66) has displayed impressive changes on short timescales. The history of these changes is described below.

First, in 1987, CS N66 had a weak (barely detectable) blue continuum (Peña & Ruiz 1988). From nebular parameters Peña et al. (1994, 1995) derived a He II Zanstra temperature $T_Z \sim 120,000$ K and a luminosity $\log(L_*/L_\odot) \sim 4.4$, which, when compared with evolutionary tracks, indicated a stellar mass of about $1 M_\odot$. In their work on N66, Dopita et al. (1993), from a photoionization structure model, derived $T_{\text{eff}} \sim 170,000$ K, $\log(L_*/L_\odot) \sim 4.5$, and a stellar mass higher than $1 M_\odot$. These estimates indicate that CS N66 is one of the most massive PN nuclei known.

Second, between 1988 and 1990, the star began a spectacular mass-loss event, showing “mild” W-R features that were first reported by Torres-Peimbert et al. (1993). Spectroscopic and photometric data presented by Peña et al. (1994) and Cowley et al. (1994) showed well-developed W-R stellar features and a strong continuum superposed on the intense nebular emission lines. Over the course of several years, the UV and optical continuum fluxes increased by factors of about 4 and 25, respectively. The high optical stellar luminosity and the W-R features were similar to those manifested by a Population I WN4.5 star (Peña et al. 1994, 1995). Remarkably, CS N66 is the only PN nucleus showing a WN-type spectrum. All other known PN nuclei that demonstrate W-R features, in the Galaxy and the Magellanic Clouds, are WC-type (Tylenda, Acker, & Stenholm 1993; Peña, Ruiz, & Torres-Peimbert 1997).

Finally, since 1993 we have followed the stellar evolution from ground-based telescopes and the *IUE* satellite. Optical and UV spectra have been obtained every 3 or 4 months

¹ Based on observations made with the NASA/ESA *Hubble Space Telescope* obtained at the Space Telescope Science Institute, which is operated by the Association of Universities for Research in Astronomy, Inc., under NASA contract NAS 5-26555.

² Instituto de Astronomía, Universidad Nacional Autónoma de México, Apdo. Postal 70-264, 04510 México D.F., Mexico.

³ Visiting Astronomer, Cerro Tololo Inter-American Observatory, Casilla 603, La Serena, Chile.

⁴ Guest Observer with the *IUE* satellite, which is sponsored and operated by NASA, ESA, and the Science and Engineering Council of the UK.

⁵ Lehrstuhl Astrophysik der Universität Potsdam, Am Neuen Palais 10, D-14469 Potsdam, Germany.

⁶ Departamento de Astronomía, Universidad de Chile, Casilla 36-D, Santiago, Chile.

⁷ Institut für Astronomie und Astrophysik, Universitäts-Sternwarte München, Scheinerstrasse 1, D-81679, München, Germany.

TABLE 1
LOG OF *HST* FOS/BLUE OBSERVATIONS

Observation	Grating	Date	Exposure Time (minutes)
Y31L0105T	G140H	1995 Dec 11	190.0
Y31L0106T	G190H	1995 Dec 11	45.0
Y31L0107T	G400H	1995 Dec 11	35.0
Y3J30106T	G140H	1996 Nov 12	63.2
Y3J30107T	G140H	1996 Nov 12	63.2
Y3J30108T	G140H	1996 Nov 13	63.2
Y3J30109T	G190H	1996 Nov 13	43.0
Y3J3010AT	G400H	1996 Nov 13	15.0
Y3J3010BT	G400H	1996 Nov 13	24.0

that have been partially reported in Peña (1995) and Peña et al. (1994, 1996, 1997). These data indicate that the strong wind has persisted for more than 7 years. During this period the stellar continuum and the emission lines have undergone important short- and long-timescale variations. A sudden and almost total disappearance of the W-R features, which lasted several weeks, occurred in 1995 August–September, followed by a new strengthening of the emission lines and continuum, just in time for *HST* Cycle 5 observations in 1995 December.

These spectacular changes have no theoretical explanation at present. The possibility that the star is undergoing a late thermal pulse was suggested by Peña et al. (1994), but the clear evidence that the stellar atmosphere is, at present, very H-deficient makes it difficult to support this suggestion. To further investigate this event, it was necessary to study the stellar spectrum isolated from the intense nebular emission. For this purpose, high spatial resolution spectrophotometric observations were carried out with *HST* during Cycles 5 and 6 from the UV to the optical wave-

TABLE 2
STELLAR CONTINUUM FLUXES

λ (Å)	F_λ (1995 December)	F_λ (1996 November)
1300	12.6	11.2
1500	10.4	9.2
1850	7.2	6.5
3300	2.1	1.7
4000	1.2	1.0

NOTE.—Fluxes in 10^{-15} ergs cm^{-2} s^{-1} Å^{-1} , not corrected for reddening.

TABLE 3
STELLAR EMISSION-LINE FLUXES

LINE	1995 DECEMBER			1996 NOVEMBER		
	F	EW (Å)	FWHM (Å)	F	EW (Å)	FWHM (Å)
N v λ 1240	50.6	42	9.6	70.4	53	9.8
N iv λ 1488	7.6:	1.8:	1.9:	...
C iv λ 1550	4.2:	4.2	10.3	7.8	8.9	12.7
He II λ 1640	70.3	71	16.0	71.8	77	14.4
N iv λ 1718	3.8	4.5	16.0	2.6	3.4	13.8
N iv λ 3484	1.2	6.9	24.3	0.87	6.0	...
He II λ 4200	1.2	11.7	38.7	0.82	9.6	36.6
He II λ 4542	1.1	12.0	41.5	0.92	11.0	35.6
N v λ 4606	0.7:	7.1	34.4	0.5:	6.4	...
He II λ 4686	11.6	130	46.7	10.5	143	42.5

NOTE.—Fluxes in 10^{-14} ergs cm^{-2} s^{-1} , not corrected for reddening.

lengths. These spectra have been combined with *IUE* and ground-based spectra from different epochs to enlarge the spectral coverage and to analyze the stellar evolution. The data have been analyzed by means of ad hoc expanding model atmospheres that provide the fundamental stellar parameters, L_* , T_* , and R_* , as well as the chemical composition, the mass-loss rate, and the wind terminal velocity.

The observations are presented in § 2. Model description and data analysis are presented in §§ 3 and 4. In § 5, we discuss the possible mechanisms that caused the outburst.

2. OBSERVATIONS

2.1. *HST* Data

Spectroscopic data of the CS were obtained from the *HST* Faint Object Spectrograph on 1995 December 11 (Cycle 5, GO program 6055) and 1996 November 12–13, (Cycle 6, GO program 6409). Since most of the nebular emission comes from a system of bright filaments, of about 1'5 in radial extent (see Dopita et al. 1993), and only faint emission is detected from a central “hole” of a few tenths of an arcsecond around the progenitor, we isolated the central star flux using the circular 0'26 aperture. In this way a stellar spectrum almost uncontaminated by nebular emission was obtained. The log of observations is listed in Table 1. The 1995 December 11 observations were carried out shortly after the 1995 August–September minimum of the stellar W-R features.

The most important stellar emission-line fluxes and continuum fluxes were measured in both *HST* spectra and are listed in Tables 2 and 3, where we include, for each line, the intensity, equivalent width, and FWHM. Only He, N, and C lines, from different ionization stages, were detected; no O line was found. The same features were detected in both *HST* spectra, taken a year apart. The set of detected lines is very similar to that present in Population I WN-type stars (cf. Hamann, Koesterke, & Wessolowski 1995) and is very different from the lines usually detected in W-R-type PN nuclei. Both *HST* calibrated spectra and details of some of the detected lines are presented in Figure 1. Although very similar, the spectra show some interesting differences. For instance, the stellar continuum is slightly weaker in 1996 November than in 1995 December (see Table 1), and the emission-line profiles, which have a complex structure and show several components at different velocities, have changed, manifesting higher blue and lower red emissions in 1996 November than in 1995 December. Some other inter-

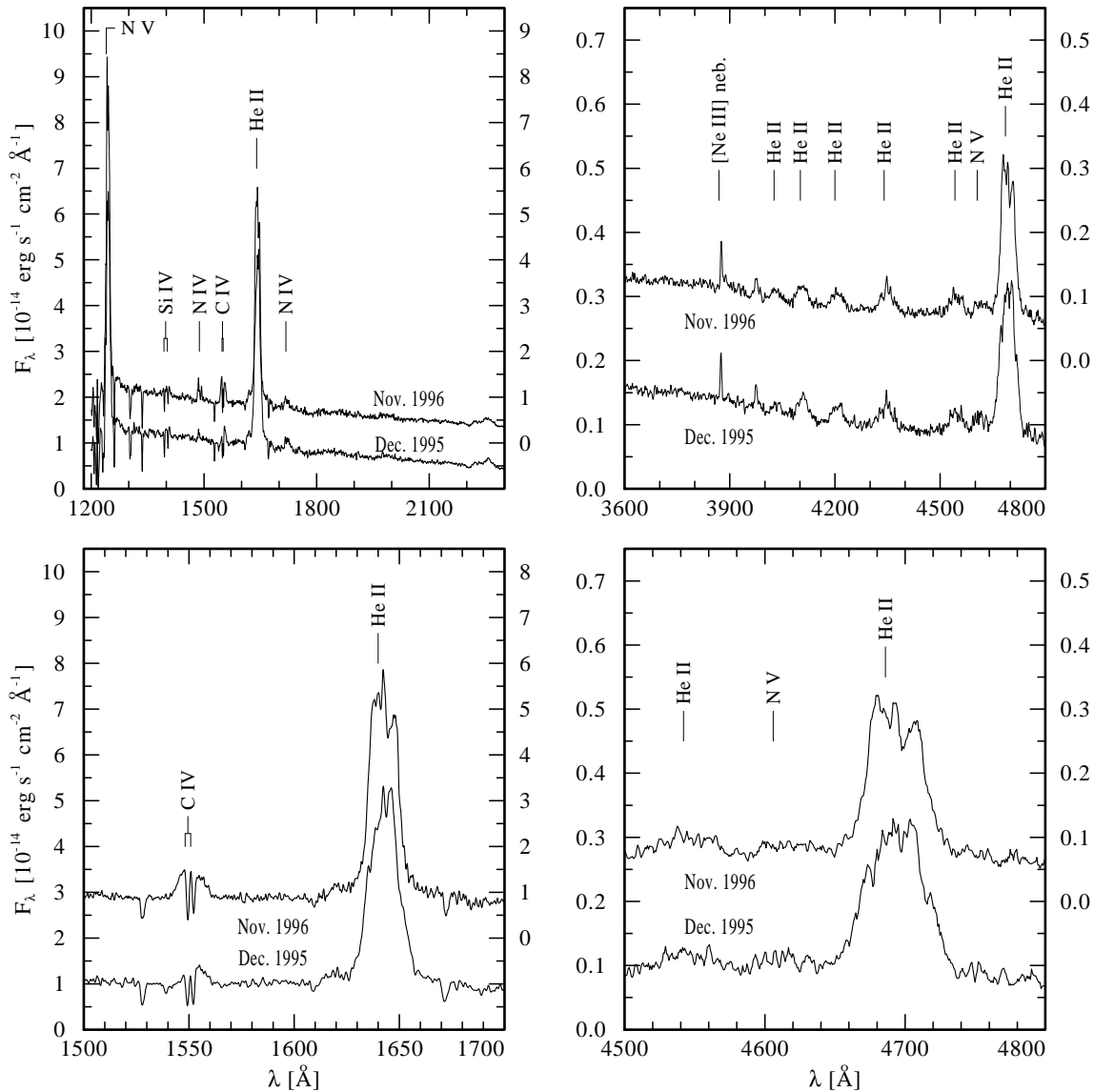


FIG. 1.—*Top*: *HST* calibrated spectra of 1995 December and 1996 November. The stellar emission was isolated using the circular $0''.26$ aperture. *Bottom*: Details of some important stellar lines are illustrated in the lower panels.

esting differences between both sets of observations are discussed in §§ 3 and 4.

2.2. IUE and Ground-based Observations

HST Cycle 5 and 6 spectra were combined with ground-based spectra obtained at Cerro Tololo Inter-American Observatory (CTIO) several weeks after the *HST* observations. The optical observations were carried out on 1996 January 23 and 1997 January 13 with the 4 m telescope equipped with the Ritchey-Chrétien spectrograph, a Loral 3K-1 CCD detector, and the KPGL No. 3 grating in first order. The wavelength range from 3650 to 7350 Å was covered with 4 Å resolution. The exposure times were 10 and 30 minutes, respectively. Both CTIO spectra were reduced using IRAF⁸ standard procedures.

In addition to the *HST* and the CTIO observations, to analyze the time evolution of the event, we have chosen (from our set of *IUE* observations) two short-wavelength,

large-aperture, low-resolution spectra obtained in different epochs: SWP 19905 (181 minutes exposure time, observed on 1983 May 5), which shows the preoutburst stellar stage, and SWP 53255 (90 minutes exposure time, obtained on 1995 January 2), showing the highest detected postoutburst stellar intensity level.

3. FITTING AN EXPANDING MODEL ATMOSPHERE TO THE DATA

Models for spherically symmetric expanding atmospheres were calculated and compared with the observed spectra in the UV and optical range. The applied code was developed by the “Potsdam group” (formerly in Kiel) and is described elsewhere (e.g., Hamann & Wessolowski 1990). These radiative transfer calculations account adequately for the extreme non-LTE situation and the velocity field. For the latter, we adopt ad hoc the usual “beta law” with $\beta = 1$, i.e., basically $v(r) = v_{\infty}(1 - R_*/r)$ (see Hamann & Schmutz 1987 for details). Helium is described as a model atom with 34 levels and 256 explicitly treated lines, while nitrogen is more complex with 90 levels and 1367 lines (528 in N III, 703

⁸ IRAF is distributed by NOAO, which is operated by AURA, Inc., under contract with the NSF.

in N iv, and 136 in N v). Dielectronic recombination processes (N iii, N iv) are also included. Line blanketing by iron-group elements cannot be accounted for in the present code. Models of the type used here have been successfully applied for quantitative spectral analyses of Population I W-R-type stars (e.g., Koesterke, Hamann, & Wessolowski 1992; Hamann, Koesterke, & Wessolowski 1993) and of WC-type central stars of PNs (Hamann 1996; Leuenhagen, Hamann, & Jeffery 1996; Koesterke & Hamann 1997).

The basic parameters that can be derived from the spectrum of a stellar wind are the following: the chemical composition, the terminal wind velocity v_∞ , the effective temperature T_* , and a quantity termed the “transformed radius” defined as R_t (Schmutz, Hamann, & Wessolowski 1989). To determine the “absolute” stellar parameters, such as L_* , R_* , and \dot{M} , the distance should be known. While this often poses problems for Galactic field stars, the location of N66 in the LMC provides a considerable advantage. For the LMC we have adopted a distance modulus of 18.45 mag⁹ (Feast & Walker 1987; Feast 1988). Note that the definition of an effective temperature is related to a reference radius by the Stefan-Boltzmann law, and different choices of that reference radius are possible in the case of spherically extended stars. In the following we will quote T_* and R_* that refer to a Rosseland optical depth $\tau_{\text{Ross}} = 20$. This R_* might be considered the radius of the hydrostatic stellar body (for a more detailed discussion, see Hamann 1994). Alternatively, we give $T_{2/3}$ and $R_{2/3}$, which hold for $\tau_{\text{Ross}} = \frac{2}{3}$.

The absence of H lines in the CS N66 spectrum implies a highly H-deficient atmosphere. From the Balmer-Pickering decrement, Peña et al. (1995) roughly estimated $X/Y \leq 0.1$. This upper limit has been confirmed by our models; therefore, the chemical composition adopted for modeling consists mostly of He with 0.4% mass fraction of N (N abundance is determined within a factor of 2). The adopted abundances reproduce well the observed stellar lines. Models including C and O were tested, and it was found that abundances $\leq 0.02\%$ by mass are consistent with the weakness of the C lines and the absence of O lines, that is to say, these elements are largely depleted in the stellar atmosphere.

The best fit to the *HST* 1996 November 6/CTIO 1997 January 13 observations (merged at 4821 Å) is presented in Figure 2. The model flux has been reddened using the LMC reddening law as given by Nandy et al. (1981) with $E_{B-V} = 0.10$ mag and scaled with the LMC distance modulus. Ground-based observations include the nebular and stellar emission; therefore, the theoretical nebular continuum flux, calculated from N66 nebular parameters, was subtracted from the CTIO spectrum ($\lambda > 4821$ Å). The best-fit model parameters, listed in Table 4, indicate that at the end of 1996, CS N66 was a highly luminous [$\log(L_*/L_\odot) = 4.53$] and hot ($T_* = 93,300$ K) He star with a small amount of N (0.4% by mass). It had a radius $R_* = 0.71 R_\odot$, and it was undergoing violent mass loss at a rate $\dot{M} = 10^{-5} M_\odot \text{ yr}^{-1}$ with a wind terminal velocity $v_\infty = 2000 \text{ km s}^{-1}$. The pseudophotosphere produced by the optically thick stellar wind was very extended ($R_{2/3} = 1.74 R_\odot$) and much cooler ($T_{2/3} = 59,300$ K) than the stellar core.

⁹ A new estimate for the LMC distance modulus of 18.65 mag has been recently reported by Feast & Catchpole (1997). If this value is confirmed, our results should be scaled accordingly.

TABLE 4
PARAMETERS FOR THE BEST-FIT MODELS

PARAMETER	EPOCH ^a		
	1983 May	1995 January	1996 November –1997 January
$\log(L_*/L_\odot)$	4.53	4.53	4.53
m_V	18.6	16.4	17.3
T_* (10^3 K)	93.3	93.3	93.3
$T_{2/3}$ (10^3 K)	93.0	40.9	59.3
R_t (R_\odot)	15.41	1.54	2.85
R_* (R_\odot)	0.71	0.71	0.71
$R_{2/3}$ (R_\odot)	0.71	3.66	1.74
$\log \dot{M}$ ($M_\odot \text{ yr}^{-1}$)	–6.1	–4.6	–5.0
v_∞ (km s^{-1})	2000	2000	2000
$T_Z(\text{H II})$ (10^3 K)	105	47	65
$T_Z(\text{He II})$ (10^3 K)	81	0	0

^a Preoutburst, highest stellar brightness, and present epochs, respectively.

On the other hand, the *HST* December 1995/CTIO January 1996 spectrum is well reproduced with an atmospheric model having the same basic stellar parameters, L_* , T_* , and R_* , but the higher flux level of this epoch (see Table 2) requires a slightly higher mass-loss rate, $\dot{M} \approx 1.6 \times 10^{-5} M_\odot \text{ yr}^{-1}$.

Models to fit the *IUE* SWP 19905 (1983 May, preoutburst epoch) and SWP 53255 (1995 January, maximum stellar brightness postoutburst) spectra were also calculated. Special care was taken in subtracting the nebular contribution to the observed continuum to perform a reliable comparison between models and observations. The best models (fitting the UV spectra and the observed visual magnitudes) are presented in Figure 3. It should be noted that the model fitting SWP 19905 predicts a faint He II $\lambda 4686$ stellar emission line that should have been marginally detected in visual observations at the time. Many authors observed N66 from 1960 to 1987, and nobody reported this stellar line; therefore, the model for SWP 19905 will be considered an upper limit for the preoutburst epoch.

The stellar parameters derived from each model are listed in Table 4. The comparison between the different epochs demonstrates that all the data are fitted with models having the same fundamental parameters L_* , T_* , and R_* , but the mass-loss rate changes from $\dot{M} \leq 8 \times 10^{-7} M_\odot \text{ yr}^{-1}$ in 1983 (preoutburst stage) to $\dot{M} = 2.5 \times 10^{-5} M_\odot \text{ yr}^{-1}$ during the highest stellar intensity level in 1995 January. That is, models indicate that in 1983, CS N66 probably had an undetectable stellar wind and that the remarkable spectral changes observed since 1990 are produced by a largely enhanced and variable mass-loss rate.

An interesting point is that when the wind is very thick, $\tau_{2/3}$ occurs far outer in the stellar photosphere (compare $R_{2/3}$ and R_* in Table 4) and most of the extreme-UV ionizing photons ($\lambda \leq 228$ Å) are absorbed in the extended envelope because of the recombination of the He^{++} . In these cases $T_{2/3}$ is much lower than T_* , and the He II Zanstra temperature predicted by the models, $T_Z(\text{He II})$, is extremely low in contrast to the value $T_Z(\text{He II}) = 81,000$ K derived for the preoutburst epoch. It is worthwhile to point out that the amount of He II-ionizing photons predicted by the model for 1983 is in good agreement with the number of photons required to produce the nebular ionic abundance ratio $\text{He}^{++}/\text{He} \approx 0.5$ observed (Peña et al. 1995). But

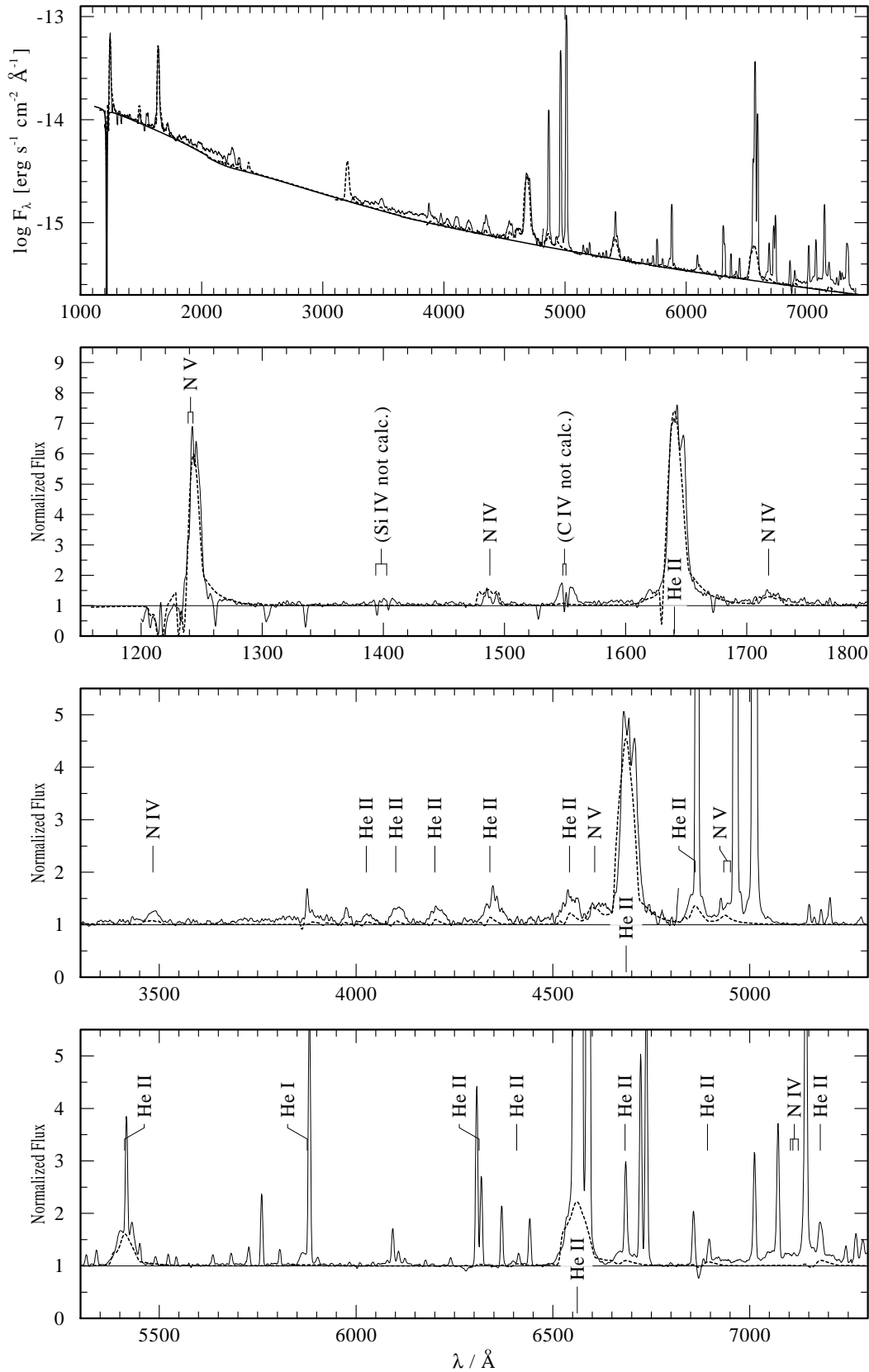


FIG. 2.—*HST* spectrum of CS N66 (1996 November 6), merged at $\lambda = 4821 \text{ \AA}$ with a CTIO spectrum (1997 January 13) compared to our best synthetic spectrum (*dashed curves*). The model parameters are given in Table 4. The synthetic spectrum is smoothed over 1 \AA (UV) and 3 \AA (optical), respectively, to match the instrumental broadening of the observations. In the top panel the model flux, reddened using the LMC reddening law (Nandy et al. 1981) with $E_{B-V} = 0.10$ mag and scaled with the LMC distance modulus (18.45 mag), is compared with the calibrated observed flux. The nebular continuum was subtracted from the CTIO spectrum ($\lambda > 4821$). The lower three panels display enlarged details in terms of normalized fluxes; the observed spectra were normalized “by eye.” The bump observed at $\lambda \geq 7000 \text{ \AA}$ is due to “blue leak” in the spectrograph.

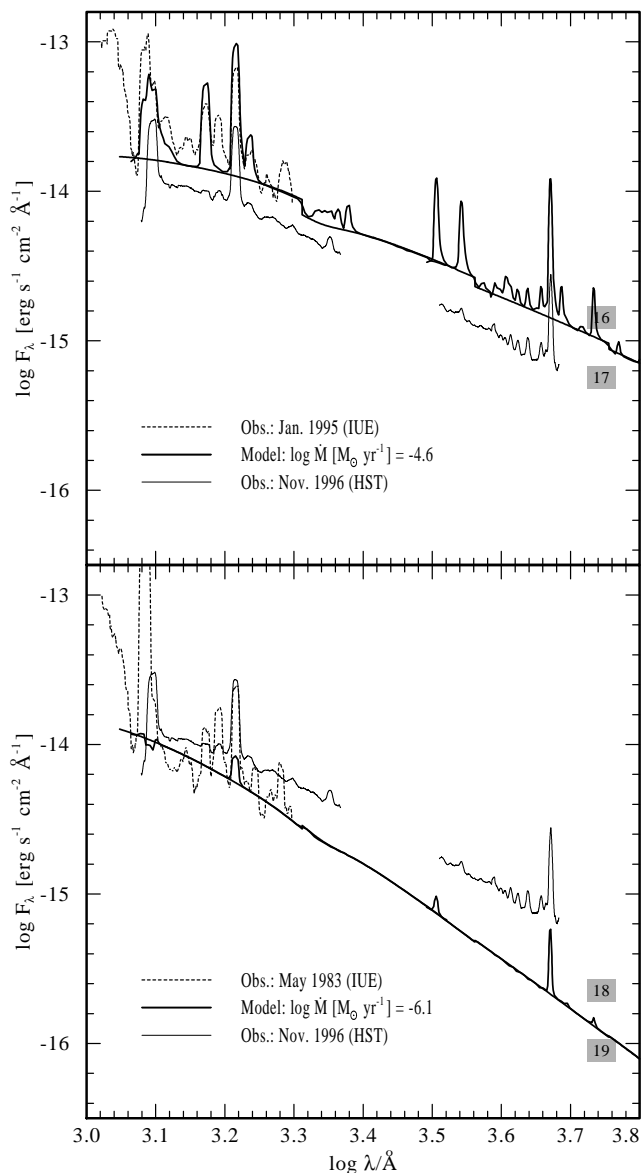


FIG. 3.—Low-resolution, large-aperture *IUE* spectra of CS N 66 (*top*, SWP 53255, 1995 January 5, 90 minutes exposure time; *bottom*, SWP 19905, 1983 April 5, 181 minutes exposure time), compared with our synthetic spectra (*thick curves*). The numbers in the blocks at $\log \lambda = 3.74$ in both panels indicate the model visual magnitude. The model parameters are given in Table 4. The synthetic spectra, reddened using the LMC reddening law (Nandy et al. 1981) with $E_{B-V} = 0.10$ mag and scaled with the LMC distance modulus, are smoothed over 8 \AA to match the instrumental broadening of the observations. The nebular continuum was subtracted from the observations. The *HST* spectrum of 1996 November 6 is included in both panels for comparison.

during the optically thick wind phase, no He II-ionizing photon escapes from the false photosphere. If this lack of energetic UV photons persists for a long time, the highly ionized species in the nebula (He II, N V, O IV, etc.) should recombine in timescales of about 30–40 yr. The presence of strong He II nebular lines also suggests that the previous history of CS N66 must have been characterized by a smaller \dot{M} than what has been observed since 1990.

4. STELLAR VERSUS NEBULAR CHEMICAL ABUNDANCES

The chemical composition derived from the model atmosphere shows an extremely H-deficient photosphere, with

$X/Y \leq 0.1$. The wind material consists mostly of helium, with a small amount of nitrogen ($\sim 0.4\%$ by mass), while carbon and oxygen are considerably depleted or absent (abundances $\leq 0.02\%$ by mass). It is evident that, at present, we are observing regions that have suffered nuclear processing during the main-sequence phase. The large depletion of C and O indicates that these elements were converted into N during the CNO cycle in the H-burning stage. The present C/O and N/O abundance ratios in the atmosphere are very similar to those reported for Population I early WN-type stars (Willis 1991), and they correspond to the equilibrium CNO nuclear burning values calculated by Maeder & Meynet (1987). There is no evidence of freshly made C brought up to the surface.

The high luminosity, large mass-loss rate, and C-poor photospheric chemical composition of CS N66 make it very different from the H-deficient PN nuclei (with or without strong winds), most of which show He-burning products (Méndez 1991; Koesterke & Hamann 1997). The rare exceptions are the nuclei of K1-27 and LoTr 4 [classified as O(He) stars by Méndez 1991], which are also almost pure He stars. Both PNs were recently analyzed by Rauch, Köppen, & Werner (1994, 1996), who found photospheric abundances very similar to those found for CS N66. Furthermore, CS K1-27 has an effective temperature of 100,000 K and a gravity $\log g = 6.5$; CS LoTr 4 has $T_{\text{eff}} = 120,000$ K and $\log g = 5.5$. Therefore, the effective temperatures are similar to T_* in CS N66, but the high gravities of these stars, compared with the gravity of CS N66, indicate less massive and much less luminous objects. Rauch et al. (1994, 1996) have interpreted these stars as “late He-flash objects” that have lost their H-rich envelopes and are showing CNO-processed material.

On the other hand, the nebular abundances in the three objects are normal. For N66, Peña et al. (1995) derived (without considering possible temperature fluctuation effects) $\text{He}/\text{H} = 0.116$, $\text{C}/\text{H} = 3.47 \times 10^{-5}$, $\text{N}/\text{H} = 8.91 \times 10^{-5}$, $\text{O}/\text{H} = 1.74 \times 10^{-4}$, and $\text{Ne}/\text{H} = 5.01 \times 10^{-5}$. These values, compared with the LMC H II region abundances (Dufour 1984, 1990), indicate moderate N enrichment and C depletion. Oxygen seems also slightly depleted, but, unlike the C depletion, the O depletion might not be real and could be due to temperature fluctuations.

Because of the importance of C, N, and O nebular abundances for understanding the CNO nuclear burning and the contamination of the atmosphere through the different dredge-up processes, we have recalculated the O abundance including temperature fluctuations. We have also recalculated the He ionic abundances to derive the ionization correction factor for the unseen ionization stages of oxygen. Furthermore, we have derived C/O and N/O abundance ratios based on the UV O III] $\lambda 1666$, C III] $\lambda 1909$, and N III] $\lambda 1750$ lines; in this way the abundance ratios are almost independent of temperature fluctuations (Garnett et al. 1995).

The relevance of temperature fluctuation effects on abundance determinations has been discussed by several authors (e.g., Peimbert 1971; Liu & Danziger 1993; Peimbert, Torres-Peimbert, & Luridiana 1995). In this work, we have adopted the prescriptions of Peimbert (1971) to derive nebular abundances considering several values for the temperature fluctuation parameter, t^2 . The optical and UV emission-line intensities reported by Peña & Ruiz (1988) and Peña et al. (1995) were used after correcting for

TABLE 5
DEREDDENED NEBULAR
LINE INTENSITIES

Line	$I_\lambda/I(H_\beta)$
O III] $\lambda 1666$	0.63
N III] $\lambda 1750$	0.99
C III] $\lambda 1909$	0.91
[O II] $\lambda 3727$	0.83
[O III] $\lambda 4363$	0.22
He II $\lambda 4686$	0.69
[O III] $\lambda 5007$	9.55
He I $\lambda 5876$	0.09

reddening; in agreement with the stellar parameters, the LMC reddening law by Nandy et al. (1981) and $E_{B-V} = 0.10$ mag were adopted. The line fluxes used are presented in Table 5.

To derive ionic abundances, a two-temperature zone scheme was adopted: the electron temperature of the high-ionization zone, $T_0(\text{high})$, was used for the doubly ionized species and He^+ , and the temperature of the low-ionization zone, $T_0(\text{low})$, was used for the singly ionized species. For the non-temperature fluctuation case, $t^2 = 0.00$, we adopted $T_0(\text{high}) = T(\text{O III}) = 16,500 \pm 200$ K, as derived from the [O III] $\lambda 1666/\lambda 5007$ and $\lambda 4363/\lambda 5007$ intensity ratios, and $T_0(\text{low}) = T(\text{O II}) = 12,300 \pm 500$ K as given by Peña et al. (1995). Furthermore, $T_0(\text{high})$ and $T_0(\text{low})$ were calculated considering $t^2 = 0.03$ and 0.06 ; they are presented in Table 6. He^{++} , He^+ , O^{++} , and O^+ ionic abundances (by number) were calculated for the different values of $T_0(\text{high})$ and $T_0(\text{low})$ from the He II $\lambda 4686$, He I $\lambda 5876$, [O III] $\lambda 5007$, and [O II] $\lambda 3727$ line intensities, respectively. The results are presented in Table 6, where we have included the He and O total abundances (by number). He abundance is the addition of He^{++} and He^+ ionic abundances and O was derived from

$$\frac{\text{O}}{\text{H}} = \left(\frac{\text{He}^+ + \text{He}^{++}}{\text{He}^+} \right) \left(\frac{\text{O}^{++} + \text{O}^+}{\text{H}^+} \right). \quad (1)$$

The ionization correction factor, $[(\text{He}^+ + \text{He}^{++})/\text{He}^+]$, has a value of 2.03, as derived from the He ionic abundances.

As expected, the He abundance determination is almost independent of temperature fluctuations, yielding an average value of $\text{He}/\text{H} = 0.118 \pm 0.001$, but the O abundance depends strongly on the t^2 -value adopted, varying

from $\text{O}/\text{H} = 1.99 \times 10^{-4}$ for $t^2 = 0.00$ to $\text{O}/\text{H} = 2.40 \times 10^{-4}$ for $t^2 = 0.06$. In the following, we will adopt $\text{O}/\text{H} = (2.20 \pm 0.20) \times 10^{-4}$ as the O nebular abundance in N66.

$\text{C}^{++}/\text{O}^{++}$ and $\text{N}^{++}/\text{O}^{++}$ ionic abundance ratios, for the three different values of t^2 , were calculated from the UV line intensities reported in Table 5 and using equations (2) and (3) presented by Garnett et al. (1995). The results are listed in Table 6. As expected, a very weak dependence of both abundance ratios with the electron temperature is found. Therefore we have adopted $\text{C}^{++}/\text{O}^{++} = 0.064 \pm 0.002$ and $\text{N}^{++}/\text{O}^{++} = 0.254 \pm 0.004$.

To obtain total abundance ratios it is necessary to correct for relative ionization volume fractions, namely:

$$\frac{\text{C}}{\text{O}} = \frac{\text{C}^{++}}{\text{O}^{++}} \frac{X(\text{O}^{++})}{X(\text{C}^{++})}, \quad (2)$$

$$\frac{\text{N}}{\text{O}} = \frac{\text{N}^{++}}{\text{O}^{++}} \frac{X(\text{O}^{++})}{X(\text{N}^{++})}. \quad (3)$$

From the photoionization structure models reported by Peña & Ruiz (1988), it is deduced that both ionization correction factors are about 1.20. Therefore, we find that $0.074 \leq \text{C}/\text{O} \leq 0.079$ and $0.30 \leq \text{N}/\text{O} \leq 0.31$. In what follows, we will adopt $\text{C}/\text{O} = 0.077 \pm 0.004$ and $\text{N}/\text{O} = 0.30 \pm 0.02$ for N66.

For the LMC H II regions, Dufour (1984, 1990) reported $\text{O}/\text{H} = (2.63 \pm 0.9) \times 10^{-4}$, $\text{C}/\text{O} = 0.32 \pm 0.10$, and $\text{N}/\text{O} = 0.035 \pm 0.015$. Therefore, within the uncertainties, we find that N66 has an O/H ratio similar to that of H II regions, while N/O is enhanced by a factor of 8.6 and C/O is depleted by a factor of 4.2. Furthermore, the $(\text{C} + \text{N})/\text{O}$ abundance ratios are equal within the uncertainties in both N66 and H II regions, indicating that in N66 most of the initial C was transformed into N during the CNO nuclear burning and that this material contaminated the atmosphere prior to the O depletion (found in the present photosphere) in the stellar interior.

That is, the chemical composition in N66 is consistent with a scenario in which the stellar atmosphere was slightly enriched with He and N produced during CNO-cycle burning, when secondary N was produced at the expense of the already existent C and brought up to the surface through the first dredge-up process, but there is no sign of any further He or N enrichment through the second dredge-up, nor of C enrichment due to the third dredge-up (see Iben

TABLE 6
CHEMICAL ABUNDANCES FOR DIFFERENT VALUES OF THE TEMPERATURE FLUCTUATION
PARAMETER t^2

Abundance ^a	$t^2 = 0.00,$	$t^2 = 0.03,$	$t^2 = 0.06,$
	$T_0(\text{high}) = 16,500$ K, $T_0(\text{low}) = 12,300$ K	$T_0(\text{high}) = 15,840$ K, $T_0(\text{low}) = 11,800$ K	$T_0(\text{high}) = 15,120$ K, $T_0(\text{low}) = 11,630$ K
He^+/H^+	0.058	0.058	0.059
$\text{He}^{++}/\text{H}^+$	0.060	0.059	0.059
He/H	0.118	0.117	0.118
$\text{O}^+/\text{H}^+ (10^{-5})$	1.70	2.19	2.51
$\text{O}^{++}/\text{H}^+ (10^{-5})$	8.13	8.71	9.33
$\text{O}/\text{H} (10^{-4})$	1.99	2.21	2.40
$\text{C}^{++}/\text{O}^{++}$	0.066	0.064	0.062
C/O	0.079	0.077	0.074
$\text{N}^{++}/\text{O}^{++}$	0.256	0.254	0.250
N/O	0.310	0.305	0.300

^a By number.

& Renzini 1983 for a discussion of dredge-up episode effects).

The differences between the nebular and stellar chemical abundances in CS N66 are commonly found in PNs with W-R nuclei. The cases reported in the literature (e.g., Gorny & Stasińska 1995; Peña et al. 1997) indicate a nebula with a “normal” chemical composition, only slightly contaminated by processed material brought up to the surface via dredge-up events, surrounding a star that exhibits highly processed material. No transition zone has been detected, except in the cases of A78 and A30, where some extremely He- and C-rich knots were found near the central stars (e.g., Jacoby & Ford 1983).

5. THERMAL PULSE VERSUS ATMOSPHERIC INSTABILITY

To understand the phenomenon occurring in N66, it is important to follow the evolution of the stellar luminosity. Expanding atmosphere models, fitting the observations of different epochs, indicate that L_* has not changed substantially since 1983. As derived from the models, the luminosity, the stellar temperature, and the radius remain approximately constant in time, showing values of $\log(L_*/L_\odot) = 4.53 \pm 0.10$, $T_* = 93,300 \pm 3000$ K, and $R_* = 0.71 R_\odot$ in all the models. $T_{2/3}$ and $R_{2/3}$, however, do indeed change with the mass-loss rate. It should be noted that L_* derived from the stellar spectrum is equal, within the uncertainties, to the luminosity values estimated by different authors from nebular parameters (e.g., Dopita et al. 1993; Peña et al. 1995).

Therefore, we determined that the essential characteristics of CS N66 have not changed significantly. The remarkable long- and short-term variations observed in the stellar continuum (for instance, the differences between the two sets of *HST* observations) and the development and disappearance of strong W-R features can be explained by substantial fluctuations in the mass-loss rate, which, according to models, varied from $\dot{M} \leq 8 \times 10^{-7} M_\odot \text{ yr}^{-1}$ in 1983 (preoutburst epoch) to $\dot{M} = 2.5 \times 10^{-5} M_\odot \text{ yr}^{-1}$ in early 1995, when the star displayed the maximum brightness and strongest W-R features. The same explanation, applied to the fast stellar fading and subsequent strengthening that occurred in 1995 August–September, indicates that these variations by a factor of 30 in the mass-loss rate can occur in timescales of a few weeks.

Concerning the possible physical mechanism that caused the outburst, a late thermal pulse has become very objectionable, because we have confirmed that the surface chemical composition of the central star is extremely H-deficient; therefore we do not expect any internal H to be present. For the same reason (absence of H at the surface), we can rule out a reignition of a H-rich shell as the triggering event.

Furthermore, the approximately constant values of the stellar parameters, L_* , T_* , and R_* , over all the evolution of the outburst and in the preoutburst epoch, indicate that, contrary to the initial expectations, there is no convincing evidence that the central star has begun a loop in the H-R diagram as was predicted for “thermal pulse” events (characterized by a large initial drop in luminosity; e.g., Schönberner 1983). Vassiliadis (1996) has also had difficulty in reconciling the light curve of the stellar continuum at 5000 Å with the predictions of thermal pulse evolutionary tracks.

The outburst in CS N66 is in some sense similar to the giant eruptions of luminous blue variables (LBVs; see, e.g.,

Davidson, Moffat, & Lamers 1989) like η Carinae or P Cygni. Of course CS N66 is quite different: much smaller mass, radius, and luminosity and a much higher effective temperature. Nevertheless, it is natural to think that, given its position in the $\log L$ – $\log T_{\text{eff}}$ diagram, which is very close to the Eddington limit adequate to its mass, CS N66 is suffering a similar kind of instability related to the strong radiation pressure.

In the case of LBVs, these massive stars are believed to be approaching the Eddington limit as they evolve toward lower temperatures (e.g., Lamers & Fitzpatrick 1988), and therefore they are moving toward a more unstable region of the H-R diagram. Additionally, recent models have shown that these massive stars can be violently unstable to non-radial pulsations (Kiriakidis, Fricke, & Glatzel 1993; Gautschy & Saio 1996; Glatzel & Mehren 1996), demonstrating a probable connection between “strange mode instabilities” and short-term variabilities in LBVs, with typical timescales of days to weeks.

In the case of post-AGB (asymptotic giant branch) stars, H-burning evolution models indicate that the stars are roughly moving at constant luminosity, following a track parallel to the Eddington limit as they evolve toward higher temperatures. For He burners near $T_{\text{eff}} \approx 100,000$ K (as the case of CS N66) evolutionary tracks (Blöcker 1995) show that the stars are slowly moving away from the Eddington limit as they evolve towards higher temperatures. This would imply that CS N66 is becoming more stable as it evolves and that radiation pressure alone is not enough to produce the eruption. Nevertheless, all these models refer to stars that still have an H-rich atmosphere and are much less massive and luminous than CS N66, and therefore, they might not be adequate in this case.

Analyzing the Eddington limit instability, the radiation pressure on electrons over gravity Γ , can be expressed as

$$\Gamma = \frac{3.09 \times 10^{-5} q L_*}{M_*}, \quad (4)$$

where L_* and M_* are given in solar units and q is the number of free electrons per atomic mass unit. In a restricted sense, the Eddington limit is where $\Gamma = 1$. In the case of CS N66 it is not easy to predict how the total opacity might behave. However, considering only electron-scattering opacity, a slowly decreasing mass (through mass loss) joined to an increasing ionization (increasing opacity) while the star evolves toward higher T_{eff} could have caused the star to approach the Eddington limit, triggering the large mass-loss event.

Another, more likely triggering mechanism, perhaps helped by the strong radiation pressure, is that, as in the case of massive stars, CS N66 has recently entered a region of enhanced instability in the H-R diagram. It would be worthwhile to explore the possibility of similar nonradial pulsational instability regions near the present position of CS N66 in the H-R diagram that might trigger strong, long-timescale eruptive events if helped by the relatively high radiation pressure in such an extremely massive central star of PN.

The theoretical problem is far from simple, because to perform a reliable stability analysis it is necessary to know the internal structure and chemical composition of this kind of H-deficient post-AGB star, whose evolutionary history cannot yet be calculated with full consistency. Probably, a

long study will be required before a satisfactory understanding of this eruptive episode in N66 is achieved. On the observational side, it is clear that the evolution of this unique object should be followed very carefully. We do not expect to find many of these massive central stars at such a high luminosity, and this may be the only chance we have for quite a long time to come.

Helpful assistance during *HST* observations provided by H. Lanning and the staff members is deeply appreciated. We

acknowledge useful discussions with A. W. Fullerton, R.-P. Kudritzki, and W. Glatzel. This work received partial support from DGAPA, UNAM (grants IN 100693 and IN 109696) and CONACYT, Mexico (F-113-E9201). R. H. M. acknowledges support by the Deutsche Forschungsgemeinschaft through grant SFB (Sonderforschungsbereich) 375. M. T. R. acknowledges financial support from FONDECYT (grant 19505880) and Cátedra Presidencial en Ciencias 1996.

REFERENCES

- Blöcker, T. 1995, *A&A*, 299, 755
 Cowley, A., Crampton, D., Schmitdke, P. C., McGrath, T. K., & Hutchings, J. B. 1994, *PASP*, 106, 876
 Davidson, K., Moffat, A. F. J., & Lamers, H. J. G. L. M., eds. 1989, *IAU Colloq. 113, Physics of Luminous Blue Variables* (Dordrecht: Kluwer)
 Dopita, M. A., Ford, H. C., Bohlin, R., Evans, I. N., & Meatheringham, S. J. 1993, *ApJ*, 418, 804
 Dufour, R. J. 1984, in *IAU Symp. 108, Structure and Evolution of the Magellanic Clouds*, ed. S. van den Bergh & K. S. de Boer (Dordrecht: Reidel), 353
 ———. 1990, in *Evolution in Astrophysics*, ed. E. J. Rolfe (ESA SP-310) (Paris: ESA), 117
 Feast, M. W. 1988, in *ASP Symp. 100, The Extragalactic Distance Scale*, ed. S. van den Bergh & C. J. Pritchett (San Francisco: ASP), 4
 Feast, M. W., & Catchpole, R. M. 1997, *MNRAS*, 286, L1
 Feast, M. W., & Walker, A. R. 1987, *ARA&A*, 25, 345
 Garnett, D., Skillman, E., Dufour, R., Peimbert, M., Torres-Peimbert, S., Terlevich, R., Terlevich, E., & Shields, G. 1995, *ApJ*, 443, 64
 Gautschi, A., & Saio, H. 1996, *ARA&A*, 34, 551
 Glatzel, W., & Mehren, S. 1996, *MNRAS*, 282, 1470
 Gorny, S. K., & Stasińska, G. 1995, *A&A*, 303, 893
 Hamann, W.-R. 1994, *Space Sci. Rev.*, 66, 237
 ———. 1996, *Ap&SS*, 238, 31
 Hamann, W.-R., Koesterke, L., & Wessolowski, U. 1993, *A&A*, 274, 397
 ———. 1995, *A&AS*, 113, 459
 Hamann, W.-R., & Schmutz, W. 1987, *A&A*, 174, 173
 Hamann, W.-R., & Wessolowski, U. 1990, *A&A*, 227, 171
 Iben, I., & Renzini, A. 1983, *ARA&A*, 21, 271
 Jacoby, G. H., & Ford, H. C. 1983, *ApJ*, 266, 298
 Kiriakidis, M., Fricke, K. J., & Glatzel, W. 1993, *MNRAS*, 264, 50
 Koesterke, L., & Hamann, W.-R. 1997, in *IAU Symp. 180, Planetary Nebulae*, ed. H. Habing & H. Lamers (Dordrecht: Kluwer), in press
 Koesterke, L., Hamann, W.-R., & Wessolowski, U. 1992, *A&A*, 261, 535
 Lamers, H., & Fitzpatrick, E. 1988, *ApJ*, 324, 279
 Leuenhagen, U., Hamann, W.-R., & Jeffery, C. S. 1996, *A&A*, 312, 167
 Liu, X. W., & Danziger, I. J. 1993, *MNRAS*, 263, 256
 Maeder, A., & Meynet, G. 1987, *A&A*, 182, 243
 Méndez, R. H. 1991, in *IAU Symp. 145, Evolution of Stars*, ed. G. Michaud & A. Tutukov (Kluwer: Dordrecht), 37
 Nail, V. M., & Shapley, H. 1955, *Proc. Natl. Acad. Sci.*, 41, 685
 Nandy, K., Morgan, D. H., Willis, A. J., Wilson, R., & Gondhalekar, P. M. 1981, *MNRAS*, 196, 955
 Peimbert, M. 1971, *Bol. Obs. Tonantzintla y Tacubaya*, 6, 29
 ———. 1978, in *IAU Symp. 76, Planetary Nebulae: Observations and Theory*, ed. Y. Terzian (Dordrecht: Reidel), 215
 Peimbert, M., Torres-Peimbert, S., & Luridiana, V. 1995, *Rev. Mexicana Astron. Astrofis.*, 31, 131
 Peña, M. 1995, *Rev. Mexicana Astron. Astrofis.*, 3, 215
 Peña, M., Peimbert, M., Torres-Peimbert, S., Ruiz, M. T., & Maza, J. 1995, *ApJ*, 441, 343
 ———. 1996, *Ap&SS*, 238, 55
 Peña, M., & Ruiz, M. T. 1988, *Rev. Mexicana Astron. Astrofis.*, 16, 55
 Peña, M., Ruiz, M. T., & Torres-Peimbert, S. 1997, *A&A*, 324, 674
 Peña, M., Torres-Peimbert, S., Peimbert, M., Ruiz, M. T., & Maza, J. 1994, *ApJ*, 428, L9
 Rauch, T., Köppen, J., & Werner, K. 1994, *A&A*, 286, 543
 ———. 1996, *A&A*, 310, 613
 Sanduleak, N. 1977, *Inf. Bull. Variable Stars*, No. 1300
 Schmutz, W., Hamann, W.-R., & Wessolowski, U. 1989, *A&A*, 210, 236
 Schönberner, D. 1983, *ApJ*, 272, 708
 Torres-Peimbert, S., Peimbert, M., Ruiz, M. T., & Peña, M. 1993, in *IAU Symp. 155, Planetary Nebulae*, ed. R. Weinberger & A. Acker (Dordrecht: Kluwer), 584
 Tylenda, R., Acker, A., & Stenholm, B. 1993, *A&AS*, 102, 595
 Vassiliadis, E. 1996, *ApJ*, 465, 748
 Willis, A. J. 1991, in *IAU Symp. 145, Evolution of Stars*, ed. G. Michaud & A. Tutukov (Dordrecht: Kluwer), 195